Supplementary Information

Formation of Benzene and Naphthalene through Cyclopentadienyl-Mediated Radical-Radical Reactions

Ralf I. Kaiser[a,*], Long Zhao[a], Wenchao Lu[b], Musahid Ahmed[b,*], Marsel V. Zagidullin[c], Valeriy N. Azyazov[c], Alexander M. Mebel[d,*]

[a] *Department of Chemistry, University of Hawaii at Manoa, Honolulu, HI 96822, USA*
[b] *Chemical Sciences Division, Lawrence Berkeley National Laboratory, Berkeley, CA 94720, USA*
[c] *Lebedev Physical Institute, Samara Branch, Samara 443011, Russian Federation*
[d] *Department of Chemistry and Biochemistry, Florida International University, Miami, Florida 33199, USA*

---

[*] Corresponding author: Ralf I. Kaiser ralfk@hawaii.edu, mahmed@lbl.gov, mebela@fiu.edu

Methods

The experiments were conducted at the Chemical Dynamics Beamline (9.0.2) of the Advanced Light Source (ALS) utilizing a resistively-heated silicon carbide (SiC) chemical reactor interfaced to a molecular beam apparatus operated with a Wiley-McLaren reflectron time-of-flight mass spectrometer (Re-TOF-MS).[1-6] The chemical reactor mimics the high temperature conditions present in circumstellar envelopes of carbon stars and in combustion systems. The cyclopentadienyl radical ($C_5H_5^{\bullet}$) and the methyl radical ($CH_3^{\bullet}$) were prepared *in situ* via pyrolysis of the anisole ($C_6H_5OCH_3$; Sigma-Aldrich). The reactants were seeded at a level of 0.02 % in helium carrier gas (300 Torr) and introduced into a resistively heated silicon carbide tube (SiC) with the temperature of 1525 ± 5 K monitored using a Type-C thermocouple. The products formed in the reactor were expanded supersonically and passed through a 2 mm diameter skimmer located 10 mm downstream of the pyrolytic reactor and enter into the main chamber, which houses the Re-TOF-MS. The quasi-continuous tunable vacuum ultraviolet (VUV) light from the Advanced Light Source intercepted the neutral supersonic molecular beam perpendicularly in the extraction region of Re-TOF-MS. VUV single photon ionization is essentially a fragment-free ionization technique and hence is characterized as a *soft ionization* method.[7] The ions formed via photoionization are extracted and detected by a multichannel plate detector. Photoionization efficiency (PIE) curves, which report ion counts as a function of photon energy ranged from 8.00 to 10.00 eV, with a step interval of 0.05 eV at a well-defined mass-to-charge ratio (*m/z*), were produced by integrating the signal recorded at the specific *m/z* for the species of interest.

Supplementary Information Introduction – Theoretical Calculations

The reaction of cyclopentadienyl and methyl radicals was considered in a number of theoretical studies.[8-11] Melius at al.[8] were first to propose that the C_5H_5 + CH_3 reaction represents a potential source of benzene, as they computed the reaction pathways resulting in the formation of fulvene and various C_6H_7 isomers using the BAC-MP4 and BAC-MP2 methods. Next, Moskaleva at al.[9] investigated the pertinent C_6H_8 and C_6H_7 potential energy surfaces (PES) in more detail using more accurate ab initio G2M(rcc,MP2) and B3LYP/6-311G(d,p) methods; this work also found several reaction pathways leading to the formation of fulvene. Sharma and Green[11] calculated high-pressure-limit and pressure-dependent rate constants using RRKM–Master Equation theory and thermochemical parameters obtained using the CBS-QB3 level of quantum chemical calculations for the c-C_5H_5 + CH_3 system focusing mostly on the C_6H_8 PES and characterizing various C_6H_7 + H and $C_5H_4CH_2$ + H_2 product channels. Also, Jasper and Hansen have explored the C_6H_7 PES in relation to the kinetics of H-assisted isomerization of fulvene to benzene.[12] In the most recent study,[10] the formation of fulvene and benzene through the c-C_5H_5 + CH_3 reaction with ensuing dissociation of its primary C_6H_7 products have been explored using up-to-date chemically accurate ab initio methods and theoretical kinetics calculations employing the RRKM-ME approach. The kinetic scheme combining the primary and secondary reactions was used to generate the overall rate constants for the production of fulvene and benzene and their branching ratios in the two-step reaction sequence, c-C_5H_5 + CH_3 → C_6H_8 → C_6H_7 + H and C_6H_7 → C_6H_6 + H. The calculated results corroborated the conclusion from the earlier works that a five-member ring can be efficiently transformed into an aromatic six-member ring by methylation and provided temperature- and pressure-dependent rate constants for individual reaction channels and product branching ratios; these computationally predicted pathways are utilized in the CFD modeling in the present study.

Thus far, there has been no experiment under high temperature conditions that has monitored both the kinetics *and* elementary mechanisms of the cyclopentadienyl RSFR reacting with a second hydrocarbon radical *in situ* with mass growth processes limited to the very first aromatic

ring (Table S1). *First*, previous experiments exploited predominantly an *ex-situ* analysis of the products via gas chromatography coupled with mass spectrometry (GC-MS). This approach cannot detect unstable species and reactive intermediates, but can identify in the ex-situ mode only closed shell molecules which are thermally stable at room temperature. Therefore, the molecules detected by GC-MS are not necessarily the nascent reaction products of radical-radical reactions. *Second*, *in situ* identification of products was conducted at cyclopentadienyl radical concentrations, which were too high to eliminate mass growth processes beyond benzene and naphthalene, respectively. These high-density environments do not allow the extraction of the reaction mechanisms leading to the formation of the *initial* aromatic product since successive reactions can convert benzene and its isomers to higher molecular mass growth products.

In detail, the recombination of two cyclopentadienyl radicals was considered by the combustion community as a potential source of naphthalene via the $C_5H_5 + C_5H_5 \rightarrow C_{10}H_8 + H_2/2H$ reaction. Melius and coworkers[8] again were the first to investigate the PES for $C_5H_5 + C_5H_5$ theoretically and to propose that naphthalene can be formed through a two-step sequence involving a loss of an H atom from the initial C_5H_5-C_5H_5 complex forming the 9-H-fulvalenyl radical followed by isomerization of this radical via a so-called spiran mechanism and another H atom loss leading to naphthalene. Later, Kislov and Mebel[13] investigated isomerization and dissociation pathways of the 9-H-fulvalenyl radical in detail considering not only the spiran isomerization pathway, but additionally, a large variety of the decomposition channels to fulvalene and azulene and the methylene walk pathway reforming the azulene core in $C_{10}H_9$ to the naphthalene core. The authors also computed rate constants for the elementary reaction steps at the high-pressure limit and deduced naphthalene as the major 9-H-fulvalenyl decomposition product at low temperatures ($T < 1000$ K), with fulvalene prevailing at higher temperatures and azulene being only minor products at all conditions. Mebel and Kislov[14] also studied the $C_{10}H_{10}$ PES and showed that H_2 elimination from $C_{10}H_{10}$ is not competitive, and the initial C_5H_5-C_5H_5 complex most likely decomposes to 9-H-fulvalenyl + H. Afterwards, Cavallotti and Polino[15] revisited the $C_5H_5 + C_5H_5$ reaction and found 1-H- and 2-H-fulvalenyl radicals as well as 1-H- and 2-H-azulyls among the potential products, in addition to 9-H-fulvalenyl. Their RRKM-ME

and VTST calculations allowed the authors to evaluate temperature- and pressure-dependent rate constants and to conclude that both H-fulvalenyl and H-azulyl product channels are competitive, with the azulyl channel being preferable over the fulvalenyl pathway up to 1450 K. At last, the most detailed theoretical study of the kinetics of the $C_5H_5 + C_5H_5$ reaction and consequent decomposition of its $C_{10}H_9$ radical products was reported by Green and coworkers.[16] In particular, they took into account collisional stabilization of the $C_{10}H_{10}$ species, which appeared to be important at low and intermediate temperatures and is followed by H abstraction leading to the formation of $C_{10}H_9$ species. The detailed mechanism and rate constants by Green and co-workers are directly utilized in the present CFD modeling.

Supplementary Information Introduction – Experiments

For the reaction between cyclopentadienyl and the methyl radical (Table S1), McEnally and Pferrerle [17] performed an experimental investigation on a methane/air co-flowing non-premixed flame doped separately with C5 ring-containing compounds including cyclopentane and cyclopentene within the temperature range from 900 to1740 K and a pressure of 750 Torr. In their experiment, cyclopentene was suggested to be converted to benzene by dehydrogenation to cyclopentadienyl, reaction of the cyclopentadienyl with methyl radical to form methylcyclopentadienyl, and dehydrogenation/isomerization of the methylcyclopentadienyl to benzene; however, no experimental evidence was provided. Lindstedt and Rizos[18] explored the role of cyclopentadienyl in the formation of aromatics by kinetic modeling the cyclopentene flames and methyl-cyclopentadiene pyrolysis in a shock tube. With rate-of-production analysis, they inferred that the route to fulvene via the methyl-cyclopentadienyl radical is an important path contributing over 25%. Djokic et al.[19] detected benzene, indene, methylindenes and naphthalene as major products in the cyclopentadiene pyrolysis utilizing a tubular continuous flow reactor in the temperature range of 873-1123 K at a pressure of 1275 Torr. The recombination reaction of cyclopentadienyl and methyl was considered in their kinetic model. Herbinet et al.[20] studied the formation of aromatic rings in the pyrolysis of cyclopentene in a jet-stirred reactor at a residence time of 1 s, a pressure of 800

Torr, and a temperature range of 773 to 1073 K. They proposed that benzene is dominantly produced via cyclopentadienyl radicals (87%). Yuan et al.[21] aimed at the reaction mechanisms of cyclopentadienyl by performing an experimental and kinetic modeling study on the pyrolysis of anisole in a flow reactor at the pressures of 30 and 760 Torr and temperatures from 850 to 1160 K proposing a reaction mechanism of cyclopentadienyl/methyl to fulvene and benzene. Baroncelli et al.[22] chose cyclopentene as a primary fuel generating cyclopentadienyl radicals in high-temperature counterflow diffusion flames at 60 Torr. The kinetic prediction of benzene was compared with the measurement considering the cyclopentadienyl/methyl mechanism. An observed benzene concentration suggested the $C_5H_5 + CH_3$ route.

Compared to the cyclopentadienyl/methyl reactions, a few experimental investigations were reported on the cyclopentadienyl recombination reaction leading to the formation of naphthalene. Filley and Mckinnon[23] utilized a quartz tubular reactor to perform an investigation on the 'dimerization' of cyclopentadienyl generating naphthalene in the temperature range of 773 to 973 K. Triphenylmethylcyclopentadiene was prepared as the precursor of cyclopentadienyl. They observed the formation of naphthalene at low temperature (823 K) and atmospheric pressure via gas chromatography. Murakami et al.[24] reported on the kinetic investigation for the self-reaction of cyclopentadienyl to naphthalene using a shock tube combined with atomic resonance absorption technique, which could detect hydrogen atoms. Trifluoromethoxybenzene was chosen as the precursor and the overall rate constant for $C_5H_5 + C_5H_5 = C_{10}H_8 + 2H$ was determined as $3.3 \times 10^{17} \exp(-135 \text{ kJ/RT})$ cm^3 mol^{-1} s^{-1}. As previously introduced, Djokic et al.[19] detected benzene, indene, methylindenes and naphthalene as major products in the cyclopentadiene pyrolysis utilizing a tubular continuous flow reactor. Additionally, they found that the fraction of PAHs increases linearly with the conversion of cyclopentadiene, indicating that the cyclopentadienyl radical might play an important role in PAHs formation; elementary reaction mechanisms were not identified in this study. Knyazev and Popov[25] studied the kinetics of the self-reaction of cyclopentadienyl radicals by laser photolysis/photoionization mass spectroscopy in the temperature region 304-600 K. The overall reaction ($C_5H_5 + C_5H_5$) rate constant yielded a strong negative temperature dependence ($k = 2.9 \times 10^{-12} \exp(+1489 \text{ K/T})$ cm^3 molecule^{-1} s^{-1}). $C_{10}H_{10}$, $C_{10}H_9$ and $C_{10}H_8$ molecules were

observed. Additionally, product analysis via chromatographic techniques indicates that two isomers of $C_{10}H_8$ were detected, e.g., naphthalene (major) and azulene (minor). As mentioned before, Yuan et al.[21] performed the experimental and kinetic modeling investigation on cyclopentadienyl. They verified the C_5H_5 + C_5H_5 rection leading to the formation of naphthalene. Additionally, they found that at higher temperatures, most of phenoxy radical is consumed through the unimolecular decomposition reaction forming cyclopentadienyl radical. More recently, Wang et al.[26] studied the oxidation of cyclopentadiene in a jet-stirred reactor under the pressure of 750 Torr and the temperatures from 623 to 1073 K with different equivalence ratios. A detailed kinetic model was also constructed to propose mechanisms to naphthalene via cyclopentadienyl self reaction; however, elementary reaction mechanisms were not identified in this study.

Table S1. Previous studies on the recombination reactions of cyclopentadienyl.

Groups	Reactor	Reaction conditions	References
McEnally and Pfefferle	burner	T = 900-1740 K, P = 750 Torr	17
Lindstedt and Rizos	shock tube	T = 1506 K, P = 201 Torr	18
Djokic et al.	flow reactor	residence time = 300-400 ms, T=873~1123 K, P = 1292 Torr	19
Herbinet et al.	jet-stirred reactor	Residence time = 1 s, T = 773-1073 K, P = 800 Torr	20
Yuan et al.	flow reactor	T = 850-1160 K, P = 30, 760 Torr	21
Baroncelli et al.	counterflow burner	P = 60 Torr	22
Filley and McKinnon	quartz tubular reactor	residence time = 2 s, T=773-973 K, P = 760 Torr	23
Murakami et al.	shock tube	T = 1510 K, P = 1140 Torr	24
Knyazev and Popov	tubular reactor	residence time = 65-140 ms, T = 301, 600 and 800 K, P = 760 Torr	25
Wang et al.	jet-stirred reactor	T = 620-1073 K, P = 750 Torr	26
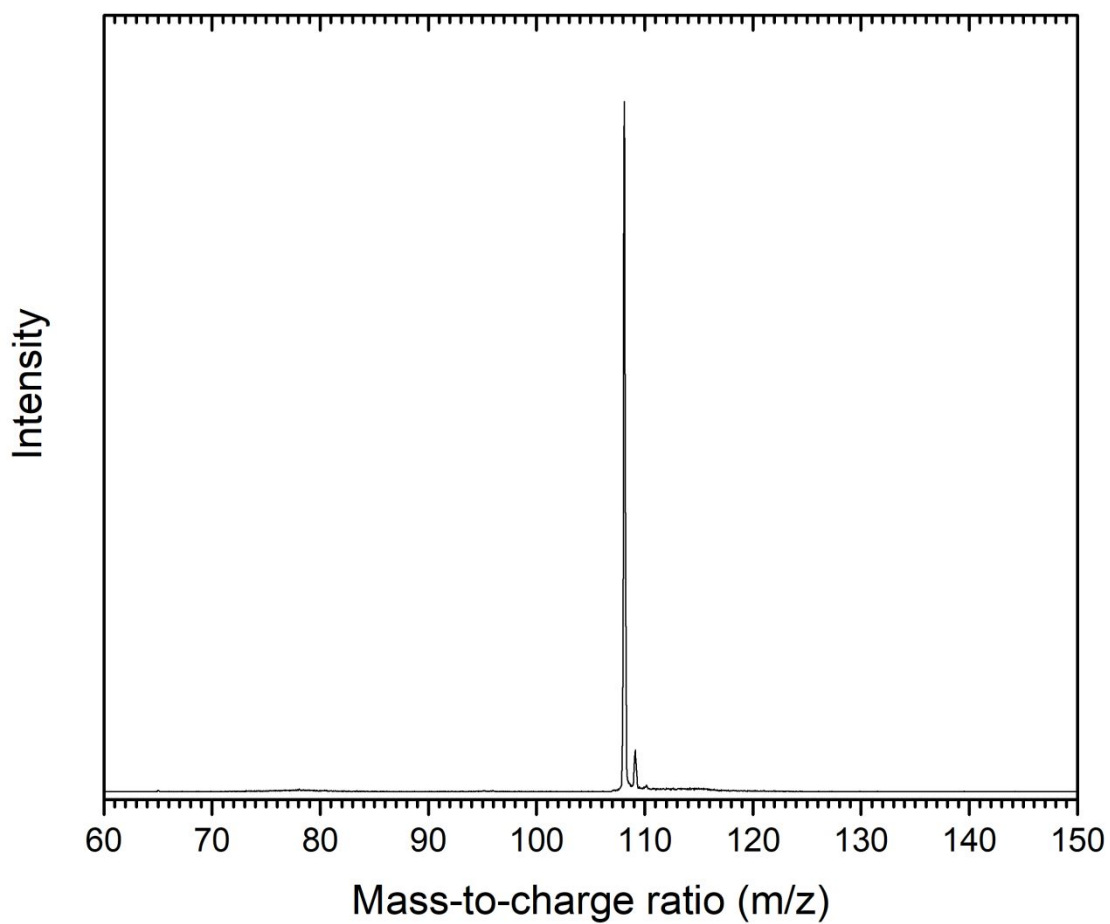
Figure S1. Photoionization mass spectrum recorded at a photon energy of 9.50 eV for the anisole/helium system with the silicon carbide tube at 293 K.
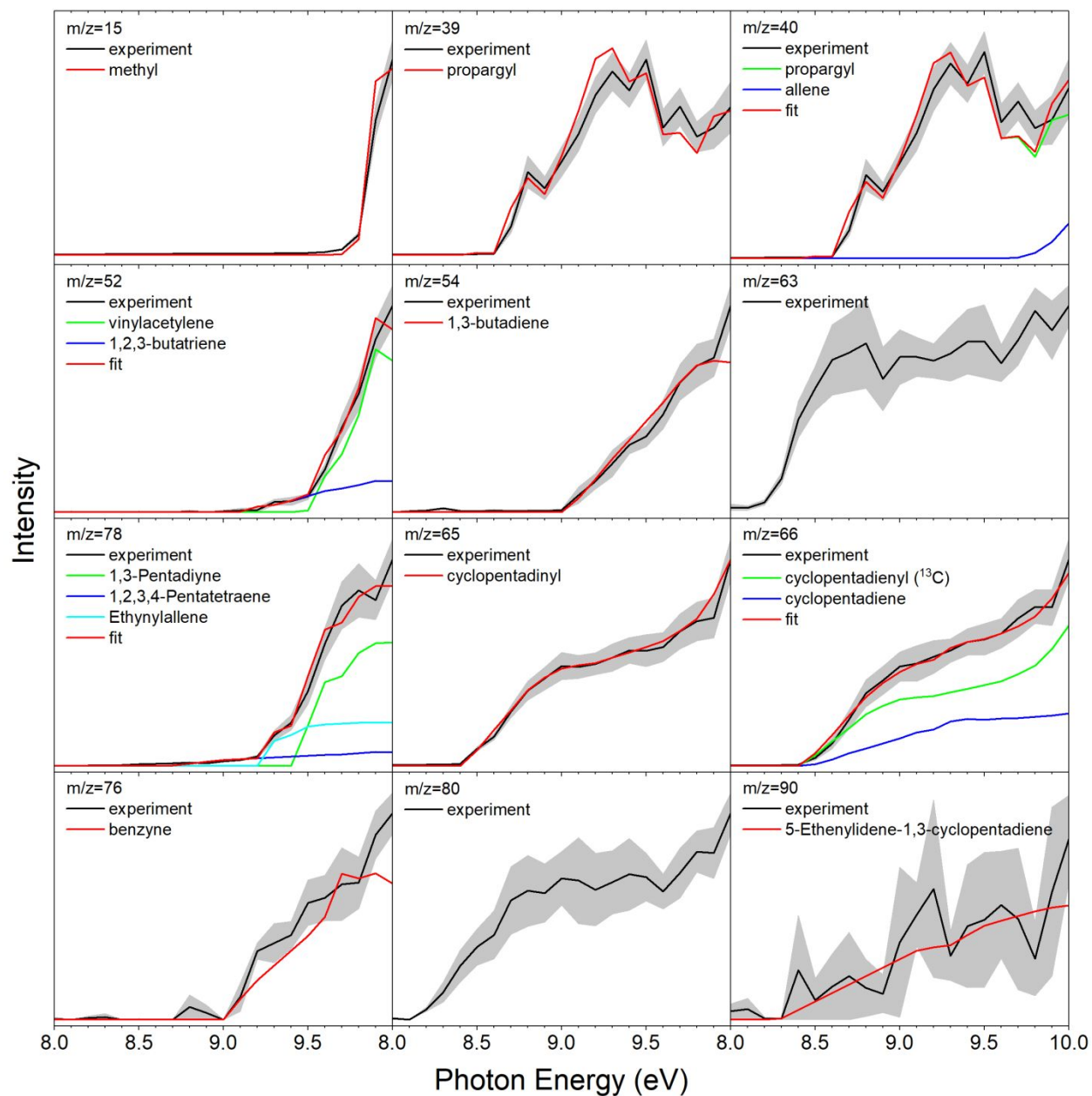
Figure S2-1. Photoionization efficiency (PIE) curves for products in the molecular beam at a reactor temperature of 1525 ± 5 K. Black: experimental data; blue/green/red: reference PIE curves; in case of multiple contributions to one PIE curve, the red line resembles the overall fit. The error bars consist of two parts: ±10% based on the accuracy of the photodiode and a 1 σ error of the PIE curve averaged over the individual scans.
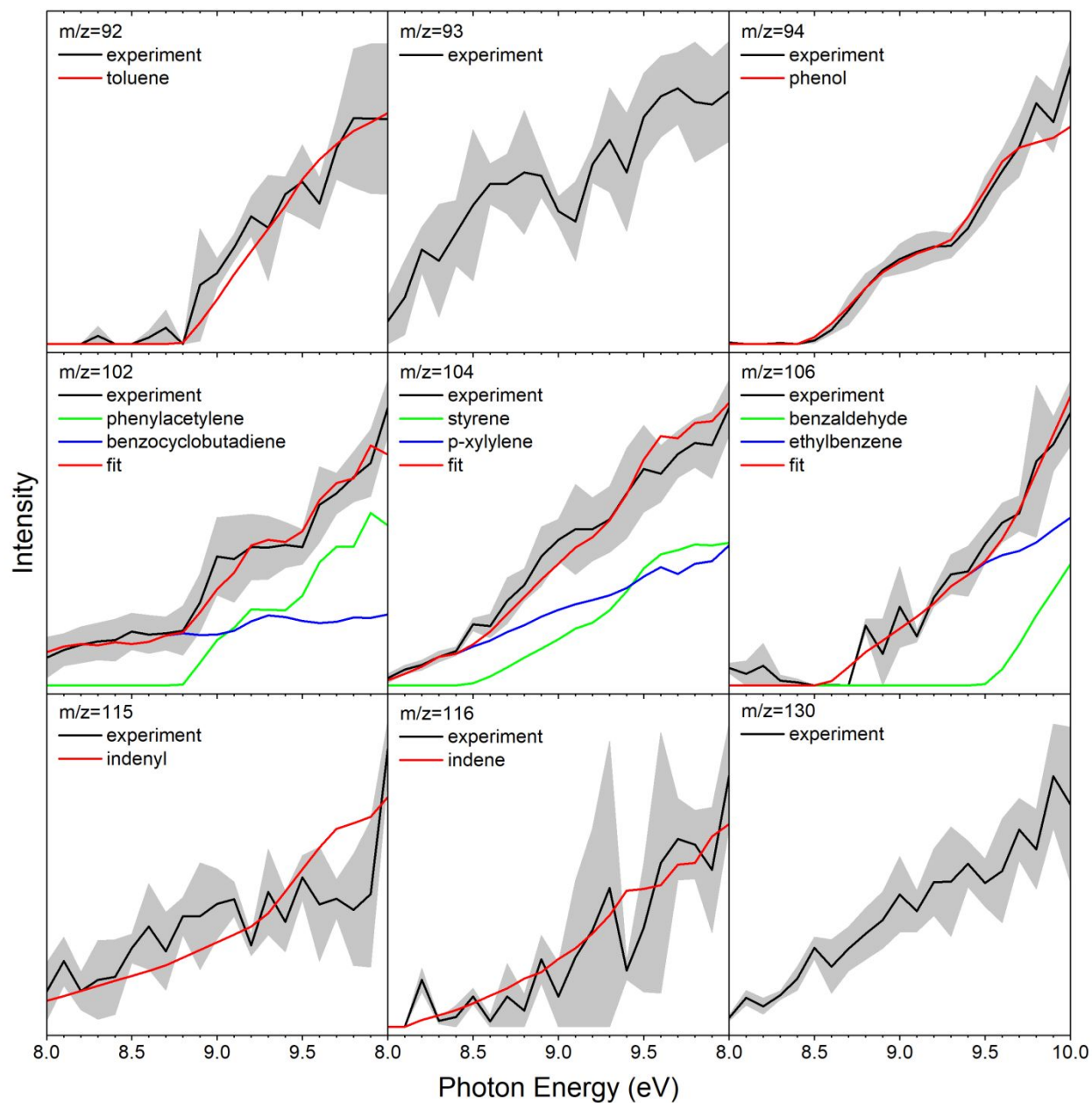
Figure S2-2. Photoionization efficiency (PIE) curves for products in the molecular beam at a reactor temperature of 1525 ± 5 K. Black: experimental data; blue/green/red: reference PIE curves; in case of multiple contributions to one PIE curve, the red line resembles the overall fit. The error bars consist of two parts: ±10% based on the accuracy of the photodiode and a 1 σ error of the PIE curve averaged over the individual scans.

Supplementary Information Discussion of PIE Curves Figure S2

The experimental PIE curve of m/z = 15 can be nicely replicated with the reference curve of the methyl radical (CH_3),[27] whereas the PIE curve at m/z = 65 can be fit with the reference curve of the cyclopentadienyl radical (C_5H_5).[28] Under our high temperature conditions in the reactor, the cyclopentadienyl radical (C_5H_5) may fragment to the propargyl radical (C_3H_3) and acetylene (C_2H_2).[26] The propargyl radical is detected through a match of the experimental PIE curve at m/z = 39 with the reference PIE curve of the propargyl radical.[27] Both the propargyl and the cyclopentadienyl radical may recombine with hydrogen atoms in the reactor to allene/methylacetylene (C_3H_4) and cyclopentadiene (C_5H_6), respectively. Here, the PIE curve at m/z = 40 can be reproduced nicely via a linear combination of PIE reference curves of ^{13}C-propargyl ($^{13}CC_2H_3$) and allene (C_3H_4). The methylacetylene isomer (CH_3CCH) has an adiabatic ionization energy of 10.36 eV and hence cannot be ionized within our photon range of 8.00 to 10.00 eV. The cyclopentadienyl radical can also undergo fragmentation by atomic hydrogen loss accompanied by isomerization; this is evident from the PIE curve at m/z = 64 and the detected C_5H_4 isomers 1,3-pentadiyne ($HCCCH_2CCH$), 1,2,3,4-pentatetraene ($H_2CCCCCH_2$), and ethynylallene ($H_2CCCCH(CCH)$). Finally, PIE curves can be extracted at m/z = 80 and 130. These m/z ratios account for molecular formulae C_6H_8 and $C_{10}H_{10}$, respectively, i.e. the molecular formulae of the methyl – cyclopentadienyl and cyclopentadienyl – cyclopentadienyl recombination. These processes lead to 5-methylcyclopenta-1,3-diene ($C_5H_5CH_3$) and 9,10-dihydrofulvalene ($C_5H_5C_5H_5$). However, no PIE reference curves are available for these isomers.

Supplementary Information Computational Fluid Dynamics Calculation Results

It is important to note that in principle, the propargyl radical self-reaction can lead to the formation of benzene (**1**), fulvene (**3**), and 1,5-hexadiyne (**4**) along with 2-ethynyl-1,3-butadiene (**5**).[29] Therefore, it is advisable to model the chemistry within the pyrolytic reactor so that potential contributions of the propargyl radical self-reaction to (**1**) and (**3**) can be explored (Table S2). The Computational Fluid Dynamics (CFD) simulations of the pyrolytic reactor included the solution of heat, momentum and mass transfer equations using Comsole Multiphysics package as described in detail in the previous work.[30] Modelling was performed to quantify the temperature and pressure distribution within the reactor (Figure S3) and the principal routes leading to experimentally detected benzene (**1**), naphthalene (**2**), fulvene (**3**), and 1,5-hexadiyne (**4**).[29] These simulations are based on the $C_5H_5 + CH_3$ and C_5H_5 recombination[10, 14] pathways (Figures 2 and 3). The list of reactions and their rate constants included in the simulation is presented in Table S2.
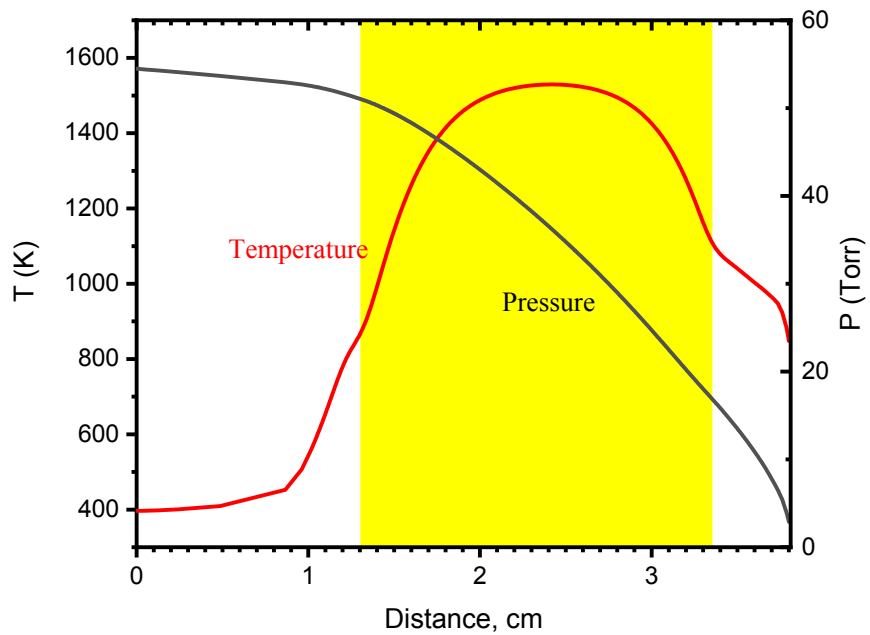
Figure S3: Centerline pressure (left y-axis) and temperature (right y-axis) along the reactor axis. The yellow shaded area defines the electrically heated section of the SiC tube. T: temperature, P: pressure.

Table S2. List of reactions and rate constants used in CFD simulation.

N	Reactions, Rate coefficient (s^{-1}, cm^3 mole^{-1} s^{-1})	P, Torr	Ref.
Reaction 1 $C_6H_5OCH_3$ (anisole) $\rightarrow$ C_6H_5O (phenoxy) + CH_3			
k1	2.0e15 ·exp(-266000/8.314/T)		[31]
Reaction 2 C_6H_5O (phenoxy) $\rightarrow$ C_5H_5 (cyclopentadienyl) + CO			
k2fp1	5.38e86·T^(-21.671) ·exp(-46200/T) + 3.46e47·T^(-10.621) ·exp(-33050/T)	7.5	[32a]
k2fp2	2.13e86*T^(-1.3138) ·exp(-28349/T) -2.48e43*T^(-8.0814) ·exp(-41058/T)	75	[32a]
k2fp3	4.18e13*T^(-013179) ·exp(-27409/T) -7.87e37*T^(-6.3299) ·exp(-41139/T)	750	[32a]
Reaction 3 C_6H_5O (phenoxy) + H $\rightarrow$ C_6H_5OH (phenol)			
k3	2.53e14		[33]
Reaction 4 C_5H_5 (cyclopentadienyl) + H $\rightarrow$ C_5H_6 (cyclopentadiene)			
k4	2.19e-10· (T/298)^0.333·exp(122/T) ·6e23	all	[34]
Reaction 5 C_5H_5 (cyclopentadienyl) $\leftrightarrows$ C_3H_3 (propargyl) + C_2H_2(acetylene)			
k5f	3.21e39 (T/298 K)^(-24.4) ·exp(-536000/8.314/T)	750	[35]
k5r	4.37e-1(T/298 K)^(-14.2) ·exp(-133000/8.314/T) ·6e23	750	[35]
Reaction 6 C_3H_3 + H $\leftrightarrows$ C_3H_4(propyne)			
k6fp1	10^36.56*T^(-7.36) ·exp(-6039/1.987/T)	30	[36]
k6fp2	10^29.90*T^(-5.06) ·exp(-4861/1.987/T)	750	[36]
k6ar	7.8e-6·exp(-335000/8.314472/T)*6.022e23	all	[37]
Reaction 7 C_3H_3 + H $\leftrightarrows$ C_3H_4(allene)			
k7fp1	5.7544e76·T^(-18.670) ·exp(-95531.0/1.987/T)	30	[36]
k7fp2	2.3442e56·T^(-12.550) ·exp(-86405.0/1.987/T)	750	[36]
k7r	3.32e-6·exp(-335000/8.314472/T) ·6.022e23	all	[37]
Reaction 8 C_3H_3 + C_3H_3 $\leftrightarrows$ C_6H_5 + H			
k8fp1	4.31E+64·T^(-15.107) ·exp(-31700/1.987/T) + 2.87E+35·T^(-6.8136) ·exp(-13327/1.987/T)	7.6	[29]
k8fp2	2.47E+66*T^(-15.446) ·exp(-36606/1.987/T) + 1.74E+35·T^(-6.7033) ·exp(-15756/1.987/T)	30	[29]
k8fp3	1.64E+64·T^(-14.71)·exp(-38110/1.987/T) + 8.00E+32*T^(-6.0398) ·exp(-16226/1.987/T)	76	[29]
k8rp1	2.73E+64·T^(-13.363) ·exp(-61451/1.987/T) + 7.91E+127·T^(-29.259) ·exp(-1.73E+05/1.987/T)	7.6	[29]
k8rp2	6.69E+63·T^(-13.074) ·exp(-64307/1.987/T)	30	[29]
k8rp3	9.98E+79·T^(-17.577) ·exp(-78756/1.987/T) + 2.07E+43·T^(-7.4005) ·exp(-52240/1.987/T)	76	[29]
Reaction 9 C_3H_3 + C_3H_3 $\rightarrow$ C_6H_6(benzene)			
k9fp1	1.19E+137·T^(-35.905) ·exp(-81665/1.987/T) + 6.87E+66·T^(-16.626) ·exp(-21855/1.987/T)	7.6	[29]

k9fp2	1.97E+103·T^(26.285) ·exp(-56243/1.987/T) + 1.84E+66·T^(-16.364) ·exp(-23047/1.987/T)	30	[29]
k9fp3	-4.85E+98vT^(-25.281) ·exp(-43301/1.987/T) + 5.24E+82·T^(-20.606) ·exp(-34270/1.987/T)	76	[29]
Reaction 10	$C_3H_3 + C_3H_3 \rightarrow C_6H_6(fulvene)$		
k10fp1	1.92E+87·T^(-22.384) ·exp(-37245/1.987/T) + 1.13E+56·T^(-13.82) ·exp(-13512/1.987/T)	7.6	[29]
k10fp2	3.86E+83·T^(-21.017) ·exp(-37704/1.987/T) + 5.28E+58·T^(-14.451) ·exp(-15599/1.987/T)	30	[29]
k10fp3	2.09E+82·T^(-20.496) ·exp(-38166/1.987/T) + 3.61E+58·T^(-14.342) ·exp(-15974/1.987/T)	76	[29]
Reaction 11	$C_3H_3 + C_3H_3 \rightarrow C_6H_6(1,5-hexadiyne)$		
k11fp1	1.76E+78·T^(-20.37) ·exp(-32169/1.987/T) + 5.51E+54·T^(-14.137) ·exp(-12026/1.987/T)	7.6	[29]
k11fp2	2.64E+61·T^(-15.268) ·exp(-22502/1.987/T) + 2.79E+47·T^(-11.604) ·exp(-9628.5/1.987/T)	30	[29]
k1fp3	8.78E+85·T^(-22.118) ·exp(-38540/1.987/T) + 2.00E+55·T^(-13.801) ·exp(-13257/1.987/T)	76	[29]
Reaction 12	$C_3H_3 + C_3H_3 \leftrightharpoons C_6H_6(2-ethynyl-1,3-butadiene)$		
k12fp1	4.00E+84·T^(-21.527) ·exp(-35767/1.987/T) + 1.89E+60vT^(-15.09) ·exp(-15352/1.987/T)	7.6	[29]
k12fp2	5.36E+82·T^(-20.74) ·exp(-37229/1.987/T) + 2.88E+55·T^(-13.495) ·exp(-14159/1.987/T)	30	[29]
k12fp3	7.41E+79·T^(-19.783) ·exp(-37027/1.987/T) + 4.92E+51·T^(-12.286) ·exp(-13002/1.987/T)	76	[29]
k12rp1	8.77E+33·T^(-6.0712) ·exp(-71073/1.987/T)	7.6	[29]
k12rp2	6.12E+29·T^(-4.8273) ·exp(-67162/1.987/T)	30	[29]
k12rp3	4.30E+39·T^(-7.6343) ·exp(-71997/1.987/T)	76	[29]
Reaction 13	$C_6H_6(1,5-hexadiyne) \rightarrow C_6H_6(fulvene)$		
k13fp1	1.40E+75·T^(-19.544) ·exp(-52706/1.987/T)	7.6	[29]
k13fp2	23.40E+61·T^(-15.232) ·exp(-48101/1.987/T)	30	[29]
k13fp3	1.48E+63·T^(-15.611) ·exp(-49730/1.987/T)	76	[29]
Reaction 14	$C_6H_6(1,5-hexadiyne) \rightarrow C_6H_6(benzene)$		
k14fp1	9.48E-55vT^(17.136) ·exp(18644/1.987/T) + 6.68E+76·T^(-19.007) ·exp(-79650/1.987/T)	7.6	[29]
k14fp2	2.86E+41·T^(-8.7) ·exp(-59368/1.987/T)	30	[29]
k14fp3	1.48E+50·T^(-10.994) ·exp(-68465/1.987/T)	76	[29]
Reaction 15	$C_6H_6(fulvene) \rightarrow C_6H_6(benzene)$		
k15fp1	1.56E+87·T^(-21.086) ·exp(-1.22E+05/1.987/T)	7.6	[29]
k15fp2	1.13E+77·T^(-18.082) ·exp(-1.17E+05/1.987/T)	30	[29]

k15fp3	7.56E+87·T^(-21.796) ·exp(-1.15E+05/1.987/T) + 1.17E+99·T^(-23.891) ·exp(-1.41E+05/1.987/T)	76	[29]
k15rp1	5.36E+87·T^(-20.781) ·exp(-1.53E+05/1.987/T)	7.6	[29]
k15rp2	6.72E+78·T^(-18.115) ·exp(-1.49E+05/1.987/T)	30	[29]
k15rp3	1.48E+90·T^(-21.905) ·exp(-1.49E+05/1.987/T) + 5.55E+104·T^(-24.972) ·exp(-1.77E+05/1.987/T)	76	[29]
Reaction 16	C_6H_6(fulvene) $\leftrightarrows$ C_6H_5 + H		
k16fp1	1.34E+91·T^(-21.678) ·exp(-1.42E+05/1.987/T)	7.6	[29]
k16fp2	1.13E+89·T^(-20.863) ·exp(-1.45E+05/1.987/T)	30	[29]
k16fp3	1.19E+87·T^(-20.178) ·exp(-1.47E+05/1.987/T)	76	[29]
k16rp1	2.64E+45·T^(-9.6881) ·exp(-23255/1.987/T) + 2.96E+87·T^(-20.902) ·exp(-57167/1.987/T)	7.6	[29]
k16rp2	3.08E+35·T^(-6.6861) ·exp(-20378/1.987/T) + 3.91E+83·T^(-19.584) ·exp(-59105/1.987/T)	30	[29]
k16rp3	2.75E+32·T^(-5.8045) ·exp(-19675/1.987/T) + 5.24E+83·T^(-19.488) ·exp(-62324/1.987/T)	76	[29]
Reaction 17	C_6H_5 +H $\leftrightarrows$ C_6H_6(benzene)		
k17fp1	4.63E+85·T^(-20.439) ·exp(-48256/1.987/T) + 5.51E+43·T^(-9.1968) ·exp(-11284/1.987/T)	7.6	[29]
k17fp2	2.90E+85·T^(-20.207) ·exp(-50909/1.987/T) + 5.09E+41vT^(-8.5303) ·exp(-10766/1.987/T)	30	[29]
k17fp3	4.63E+85·T^(-20.138) ·exp(-53321/1.987/T) + 2.08E+39·T^(-7.7679) ·exp(-10025/1.987/T)	76	[29]
k17rp1	-3.03E+71·T^(-15.07) ·exp(-1.69E+05/1.987/T) + 2.10E+43·T^(-7.7577) ·exp(-1.31E+05/1.987/T)	7.6	[29]
k17rp2	2.00E+75·T^(-16.775) ·exp(-1.54E+05/1.987/T)	30	[29]
k17rp3	9.93E+77·T^(-17.918) ·exp(-1.50E+05/1.987/T) + 2.65E+101·T^(-23.651) ·exp(-1.84E+05/1.987/T)	76	[29]
Reaction 18	C_6H_6(2-ethynyl-1,3-butadiene) $\rightarrow$ C_6H_6(fulvene)		
k18p1	1.60E+93·T^(-23.531) ·exp(-1.04E+05/1.987/T)	7.6	[29]
k18p2	4.99E+79·T^(-19.546) ·exp(-96150/1.987/T)	30	[29]
k18p3	3.80E+75·T^(-18.255) ·exp(-94952/1.987/T)	76	[29]
Reaction 19	C_6H_6(2-ethynyl-1,3-butadiene) $\rightarrow$ C_6H_6(benzene)		
k19p1	2.15E+111·T^(-28.284) ·exp(-1.25E+05/1.987/T)	7.6	[29]
k19p2	3.80E+114·T^(-28.906) ·exp(-1.33E+05/1.987/T)	30	[29]
k19p3	2.40E+100·T^(-24.769) ·exp(-1.26E+05/1.987/T)	76	[29]
Reaction 20	C_6H_6(2-ethynyl-1,3-butadiene) $\rightarrow$ C_6H_5 + H		
k20p1	5.61E+88·T^(-21.621) ·exp(-1.16E+05/1.987/T)	7.6	[29]
k20p2	8.01E+87·T^(-21.162) ·exp(-1.21E+05/1.987/T)	30	[29]
k20p3	6.84E+90·T^(-21.836) ·exp(-1.28E+05/1.987/T)	76	[29]

Reaction 21	$C_6H_6 + H \rightleftarrows C_6H_5 + H_2$		
k21f	4.57e8·T^1.88·exp(-14839/1.987/T)	all	38
k21r	1.69e4·T^2.64·exp(-4559/1.987/T)	all	38
Reaction 22	$C_6H_6(fulvene) + H \rightleftarrows C_6H_6(benzene) + H$		
k21f	6.54e25·T^(-2.8332) ·exp(-43768/1.987/T)	all	12
k21r	1.09e25·T^(-3.0678) ·exp(-11761/1.987/T)	All	12
Reaction 23 $C_5H_5 + CH_3 \rightarrow C_6H_6$ (fulvene) + 2H			
k22p1	3.64E-11·T^(-7.52E-02) ·exp(-6261.4/1.987/T)	7.5	10
k22p2	2.31E-09·T^(-4.81E-01) ·exp(-8862.0/1.987/T)	750	10
Reaction 24 $C_5H_5 + CH_3 \rightarrow C_6H_6$ (benzene) + 2H			
k23p1	4.40E-13·T^4.28E-01·exp(-2088.1/1.987/T)	7.5	10
k23p2	2.72E-10·T^(-0.44045) ·exp(-2930.3/1.987/T)	750	10
Reactions 25-359 Extended mechanism $C_5H_5 + C_5H_5 \rightarrow$ products			
	Rate constants for all elementary reactions in a complex mechanism are given as Chebyshev polynomials of T and p in CHEMKIN input file format, c5h5+c5h5_chemkin.inp		16

[a]The rate constant was computed here using the RRKM-Master Equation approach using the electronic structure data from Ref. (25).

Here, the reaction is initiated by the decomposition of the anisole precursor ($C_6H_5OCH_3$) to the methyl radical (CH_3) plus the phenoxy radical (C_6H_5O);[39] the latter decomposes to carbon monoxide (CO) plus the cyclopentadienyl radical (C_5H_5).[40] At higher temperatures, the cyclopentadienyl radical decomposes to propargyl radical (C_3H_3) and acetylene (C_2H_2).[41] The primary interest of this simulation study is to explore reactions [1] and [2] leading to benzene (**1**) and fulvene (**3**) as well as naphthalene (**2**), respectively. The second objective is to explore the contribution of the propargyl radical self-reaction leading to benzene (**1**) and 1,5-hexadiyne (**4**).[29] This led to multiple key findings as elucidated in the main manuscript. Here, since the ion count normalized by the photon fluxes holds a direct proportional relationship with the concentration, the photoionization cross section, mass discrimination, and the ion counts measured in the experiment ($S_i(T,E) \propto X_i(T) \cdot \sigma_i(E) \cdot D_i$),[7] the branching ratios between the concentrations of individual products can be calculated via ($\frac{X_i(T)}{X_j(T)} = \frac{S_i(T,E)}{S_j(T,E)} \cdot \frac{\sigma_j(E)}{\sigma_i(E)} \cdot \frac{D_j}{D_i}$). The mass discrimination factors were taken from Reference.[42]

Table S3. Photoionization cross sections (Mb) exploited in this work.

Photon Energy (eV)	Benzene[43]	Fulvene[44]	naphthalene[45]
8.5	0	9.763	5.753
9.0	0	39.548	13.982
9.5	11.048	41.893	21.720
10.0	24.282	41.893	39.125

References

(1) Zhang, F.; Kaiser, R. I.; Kislov, V. V.; Mebel, A. M.; Golan, A.; Ahmed, M., A VUV photoionization study of the formation of the indene molecule and its isomers. *J. Phys. Chem. Lett.* **2011,** *2* (14), 1731-1735.

(2) Parker, D. S.; Kaiser, R. I.; Troy, T. P.; Ahmed, M., Hydrogen Abstraction/Acetylene Addition Revealed. *Angew. Chem. Int. Ed.* **2014,** *53* (30), 7740-7744; *Angew. Chem.* **2014**, *126*, 7874-7878.

(3) Parker, D. S. N.; Kaiser, R. I.; Bandyopadhyay, B.; Kostko, O.; Troy, T. P.; Ahmed, M., Unexpected chemistry from the reaction of naphthyl and acetylene at combustion-like temperatures. *Angew. Chem. Int. Ed.* **2015,** *54* (18), 5421-5424; *Angew. Chem.* **2015**, *127*, 5511-5514.

(4) Zhao, L.; Kaiser, R. I.; Xu, B.; Ablikim, U.; Ahmed, M.; Evseev, M. M.; Bashkirov, E. K.; Azyazov, V. N.; Mebel, A. M., Low-temperature formation of polycyclic aromatic hydrocarbons in Titan's atmosphere. *Nat. Astron.* **2018,** *2* (12), 973.

(5) Zhao, L.; Kaiser, R. I.; Xu, B.; Ablikim, U.; Ahmed, M.; Zagidullin, M. V.; Azyazov, V. N.; Howlader, A. H.; Wnuk, S. F.; Mebel, A. M., VUV photoionization study of the formation of the simplest polycyclic aromatic hydrocarbon: Naphthalene ($C_{10}H_8$). *J. Phys. Chem. Lett.* **2018,** *9* (10), 2620-2626.

(6) Zhao, L.; Kaiser, R. I.; Xu, B.; Ablikim, U.; Ahmed, M.; Joshi, D.; Veber, G.; Fischer, F. R.; Mebel, A. M., Pyrene synthesis in circumstellar envelopes and its role in the formation of 2D nanostructures. *Nat. Astron.* **2018,** *2*, 413-419.

(7) Qi, F., Combustion chemistry probed by synchrotron VUV photoionization mass spectrometry. *Proc. Combust. Inst.* **2013,** *34* (1), 33-63.

(8) Melius, C. F.; Colvin, M. E.; Marinov, N. M.; Pit, W. J.; Senkan, S. M., Reaction mechanisms in aromatic hydrocarbon formation involving the C_5H_5 cyclopentadienyl moiety. *Proc. Combust. Inst.* **1996,** *26* (1), 685-692.

(9) Moskaleva, L.; Mebel, A.; Lin, M., The CH_3 + C_5H_5 reaction: A potential source of benene at high temperatures. *Proc. Combust. Inst.* **1996,** *26* (1), 521-526.

(10) Krasnoukhov, V. S.; Porfiriev, D. P.; Zavershinskiy, I. P.; Azyazov, V. N.; Mebel, A. M., Kinetics of the CH_3 + C_5H_5 reaction: A theoretical study. *J. Phys. Chem. A* **2017,** *121* (48), 9191-9200.

(11) Sharma, S.; Green, W. H., Computed Rate Coefficients and Product Yields for c-C5H5 + CH3 → Products. *The Journal of Physical Chemistry A* **2009,** *113* (31), 8871-8882.

(12) Jasper, A. W.; Hansen, N., Hydrogen-assisted isomerizations of fulvene to benzene and of larger cyclic aromatic hydrocarbons. *Proc. Combust. Inst.* **2013,** *34* (1), 279-287.

(13) Kislov, V. V.; Mebel, A. M., The formation of naphthalene, azulene, and fulvalene from cyclic C5 species in combustion: An ab initio/RRKM study of 9-H-fulvalenyl ($C_5H_5-C_5H_4$) radical rearrangements. *J. Phys. Chem. A* **2007,** *111* (38), 9532-9543.

(14) Mebel, A. M.; Kislov, V. V., Can the C_5H_5 + C_5H_5 -> $C_{10}H_{10}$ -> $C_{10}H_9$ + $H/C_{10}H_8$ + H_2 reaction produce naphthalene? An ab initio/RRKM Study. *J. Phys. Chem. A* **2009,** *113* (36), 9825-9833.

(15) Cavallotti, C.; Polino, D., On the kinetics of the C_5H_5 + C_5H_5 reaction. *Proc. Combust. Inst.* **2013,** *34* (1), 557-564.

(16) Long, A. E.; Merchant, S. S.; Vandeputte, A. G.; Carstensen, H.-H.; Vervust, A. J.; Marin, G. B.; Van Geem, K. M.; Green, W. H., Pressure dependent kinetic analysis of pathways to naphthalene from cyclopentadienyl recombination. *Combust. Flame* **2018,** *187*, 247-256.

(17) McEnally, C. S.; Pfefferle, L. D., An experimental study in non-premixed flames of hydrocarbon growth processes that involve five-membered carbon rings. *Combust. Sci. Technol.* **1998,** *131* (1-6), 323-344.

(18) Lindstedt, R. P.; Rizos, K. A., The formation and oxidation of aromatics in cyclopentene and methyl-cyclopentadiene mixtures. *Proc. Combust. Inst.* **2002,** *29* (2), 2291-2298.

(19) Djokic, M. R.; Van Geem, K. M.; Cavallotti, C.; Frassoldati, A.; Ranzi, E.; Marin, G. B., An experimental and kinetic modeling study of cyclopentadiene pyrolysis: First growth of polycyclic aromatic hydrocarbons. *Combust. Flame* **2014,** *161* (11), 2739-2751.

(20) Herbinet, O.; Rodriguez, A.; Husson, B.; Battin-Leclerc, F.; Wang, Z.; Cheng, Z.; Qi, F., Study of the formation of the first aromatic rings in the pyrolysis of cyclopentene. *J. Phys. Chem. A* **2016,** *120* (5), 668-682.

(21) Yuan, W.; Li, T.; Li, Y.; Zeng, M.; Zhang, Y.; Zou, J.; Cao, C.; Li, W.; Yang, J.; Qi, F., Experimental and kinetic modeling investigation on anisole pyrolysis: Implications on phenoxy and cyclopentadienyl chemistry. *Combust. Flame* **2019,** *201*, 187-199.

(22) Baroncelli, M.; Mao, Q.; Galle, S.; Hansen, N.; Pitsch, H. J. P. C. C. P., Role of ring-enlargement reactions in the formation of aromatic hydrocarbons. **2020,** *22* (8), 4699-4714.

(23) Filley, J.; McKinnon, J. T., Dimerization of cyclopentadienyl radical to produce naphthalene. *Combust. Flame* **2001,** *124* (4), 721-723.

(24) Murakami, Y.; Saejung, T.; Ohashi, C.; Fujii, N. J. C. l., Investigation of a new pathway forming naphthalene by the recombination reaction of cyclopentadienyl radicals. **2003,** *32* (12), 1112-1113.

(25) Knyazev, V. D.; Popov, K. V., Kinetics of the self reaction of cyclopentadienyl radicals. *J. Phys. Chem. A* **2015,** *119* (28), 7418-7429.

(26) Wang, H.; Liu, Z.; Gong, S.; Liu, Y.; Wang, L.; Zhang, X.; Liu, G., Experimental and kinetic modeling study on 1,3-cyclopentadiene oxidation and pyrolysis. *Combust. Flame* **2020,** *212*, 189-204.

(27) Savee, J. D.; Soorkia, S.; Welz, O.; Selby, T. M.; Taatjes, C. A.; Osborn, D. L., Absolute photoionization cross-section of the propargyl radical. *J. Chem. Phys.* **2012,** *136* (13), 134307.

(28) Hansen, N.; Klippenstein, S. J.; Miller, J. A.; Wang, J.; Cool, T. A.; Law, M. E.; Westmoreland, P. R.; Kasper, T.; Kohse-Höinghaus, K., Identification of C5H x isomers in fuel-rich flames by photoionization mass spectrometry and electronic structure calculations. *J. Phys. Chem. A* **2006,** *110* (13), 4376-4388.

(29) Zhao, L.; Lu, W.; Ahmed, M.; Zagidullin, M. V.; Azyazov, V. N.; Morozov, A. N.; Mebel, A. M.; Kaiser, R. I., Gas-phase synthesis of benzene via the propargyl radical self-reaction. *Sci. Adv.* **2021,** *7* (21), eabf0360.

(30) Zagidullin, M. V.; Kaiser, R. I.; Porfiriev, D. P.; Zavershinskiy, I. P.; Ahmed, M.; Azyazov, V. N.; Mebel, A. M., Functional relationships between kinetic, flow, and geometrical parameters in a high-temperature chemical microreactor. *J. Phys. Chem. A* **2018,** *122* (45), 8819-8827.

(31) Arends, I. W.; Louw, R.; Mulder, P., Kinetic study of the thermolysis of anisole in a hydrogen atmosphere. *J. Phys. Chem.* **1993,** *97* (30), 7914-7925.

(32) Tokmakov, I. V.; Kim, G.-S.; Kislov, V. V.; Mebel, A. M.; Lin, M. C., The reaction of phenyl radical with molecular oxygen: A G2M study of the potential energy surface. *J. Phys. Chem. A* **2005,** *109* (27), 6114-6127.

(33) Baulch, D. L.; Cobos, C. J.; Cox, R. A.; Esser, C.; Frank, P.; Just, T.; Kerr, J. A.; Pilling, M. J.; Troe, J.; Walker, R. W.; Warnatz, J., Evaluated Kinetic Data for Combustion Modelling. *J. Phys. Chem. Ref. Data* **1992,** *21* (3), 411-734.

(34) Harding, L. B.; Klippenstein, S. J.; Georgievskii, Y., On the combination reactions of hydrogen atoms with resonance-stabilized hydrocarbon radicals. *J. Phys. Chem. A* **2007,** *111* (19), 3789-3801.

(35) da Silva, G., Mystery of 1-vinylpropargyl formation from acetylene addition to the propargyl radical:

an open-and-shut case. *J. Phys. Chem. A* **2017,** *121* (10), 2086-2095.

(36) Miller, J. A.; Klippenstein, S. J., From the multiple-well master equation to phenomenological rate coefficients: Reactions on a C_3H_4 potential energy surface. *J. Phys. Chem. A* **2003,** *107* (15), 2680-2692.

(37) Hidaka, Y.; Nakamura, T.; Miyauchi, A.; Shiraishi, T.; Kawano, H., Thermal decomposition of propyne and allene in shock waves. *Int. J. Chem. Kinet.* **1989,** *21* (8), 643-666.

(38) Semenikhin, A.; Savchenkova, A.; Chechet, I.; Matveev, S.; Liu, Z.; Frenklach, M.; Mebel, A., Rate constants for H abstraction from benzo (a) pyrene and chrysene: a theoretical study. *Phys. Chem. Chem. Phys.* **2017,** *19* (37), 25401-25413.

(39) Lin, C.-Y.; Lin, M. C., Thermal decomposition of methyl phenyl ether in shock waves: the kinetics of phenoxy radical reactions. *J. Phys. Chem.* **1986,** *90* (3), 425-431.

(40) Carstensen, H.-H.; Dean, A. M., A quantitative kinetic analysis of CO elimination from phenoxy radicals. *Int. J. Chem. Kinet.* **2012,** *44* (1), 75-89.

(41) Mao, Q.; Huang, C.; Baroncelli, M.; Shen, L.; Cai, L.; Leonhard, K.; Pitsch, H., Unimolecular reactions of the resonance-stabilized cyclopentadienyl radicals and their role in the polycyclic aromatic hydrocarbon formation. *Proc. Combust. Inst.* **2021,** *38* (1), 729-737.

(42) Urness, K. N.; Guan, Q.; Golan, A.; Daily, J. W.; Nimlos, M. R.; Stanton, J. F.; Ahmed, M.; Ellison, G. B., Pyrolysis of furan in a microreactor. *J. Chem. Phys.* **2013,** *139* (12), 124305.

(43) Cool, T. A.; Wang, J.; Nakajima, K.; Taatjes, C. A.; Mcllroy, A., Photoionization cross sections for reaction intermediates in hydrocarbon combustion. *Int. J. Mass spectrom.* **2005,** *247* (1-3), 18-27.

(44) Osborn, D. L.; Taatjes, C. A.; Goulay, F.; Selby, T. M.; Zou, P.; Fahr, A. *A time-resolved isomer-resolved study of the propargyl self reaction using a multiplexed photoionization mass spectrometer*; Sandia National Lab.(SNL-CA), Livermore, CA (United States): 2010.

(45) Jin, H.; Yang, J.; Farooq, A., Determination of absolute photoionization cross-sections of some aromatic hydrocarbons. *Rapid Commun. Mass Spectrom.* **2020,** *34* (21), e8899.